NT@UW-20-21

Emergence of a pseudogap in the BCS–BEC crossover

Adam Richie-Halford,[1,*] Joaquín E. Drut,[2,†] and Aurel Bulgac[1,‡]

[1] *Department of Physics, University of Washington, Seattle, Washington 98195–1560, USA*

[2] *Department of Physics and Astronomy, University of North Carolina, Chapel Hill, North Carolina 27599, USA*

(Dated: May 1, 2020)

Strongly correlated Fermi systems with pairing interactions become superfluid below a critical temperature T_c. The extent to which such pairing correlations alter the behavior of the liquid at temperatures $T > T_c$ is a subtle issue that remains an area of debate, in particular regarding the appearance of the so-called pseudogap in the BCS–BEC crossover of unpolarized spin-1/2 nonrelativistic matter. To shed light on this, we extract several quantities of crucial importance at and around the unitary limit, namely: the odd-even staggering of the total energy, the spin susceptibility, the pairing correlation function, the condensate fraction, and the critical temperature T_c, using a non-perturbative, constrained-ensemble quantum Monte Carlo algorithm.

arXiv:2004.05014v2 [cond-mat.quant-gas] 29 Apr 2020

Introduction. Dilute, two-component Fermi gases with short-range interactions are relevant to a variety of systems in nuclear and condensed matter physics [1, 2]. In ultracold atomic gases [3, 4], the strength of the interaction can be tuned essentially at will by driving the system across a Feshbach resonance using an external magnetic field [5], from a weakly coupled state, well-described by Bardeen, Cooper, Schrieffer (BCS) theory, to a state with molecular bound states corresponding to a Bose-Einstein Condensate (BEC). A smooth crossover [1, 6] links these limiting regimes as one changes the sign of the inverse scattering length $1/(k_F a)$, where k_F is the Fermi momentum. On the BCS side, when $1/(k_F a) \ll -1$, pairing correlations and Cooper pairs disappear with the superconducting order parameter Δ at the critical temperature T_c. Conversely, the BEC regime, where $1/(k_F a) \gg 1$, is characterized by the pre-formation of pairs below $T^* \gg T_c$. It is common to define T^* as the temperature at which pairing correlations vanish and declare that $T^* = T_c$ on the BCS side. Between these extremes there exists a "pseudogap" regime, where one finds effects of pairing correlations *without* superfluidity and long range order for temperatures $T_c \leq T \leq T^*$. The precise scattering length at which the pseudogap regime begins is still debated [7]. Specifically, the existence of a pseudogap in the unitary limit, where $1/(k_F a) = 0$, is not settled.

Though the pseudogap is commonly defined as a suppression of the single-particle density of states near the Fermi surface, there are several competing definitions, whose differing signatures have led to debates about their respective existence [7]. The pseudogap should be identifiable from measurement of the single-particle spectrum, spin-susceptibility, and even-odd energy staggering, among others. Even when researchers agree on the definition and observable signature, there are still subjective judgements regarding the size of the effects. For example, how much suppression of the spin susceptibility, or how much even-odd energy staggering above T_c, is necessary to claim evidence for a pseudogap. As argued by Mueller [7], the main challenge in understanding and even defining the pseudogap is that one is dealing with a strongly correlated system in the normal phase.

We offer perspective on this issue by studying pseudogap signatures for $0.0 \leq 1/(k_F a) \leq 0.3$. We expect to see such signatures for the highest couplings and then detect either their disappearance or maintenance as we approach unitarity from the BEC side. We perform auxiliary-field quantum Monte Carlo (AFQMC) lattice simulations with constrained ensembles using particle-projection methods, with a previously introduced model and method [8, 9], modified to employ a cubic (rather than spherical) momentum cutoff. In addition to previously employed projections for the total particle number, we introduce a new projection for the particle asymmetry only, which is free of the infamous sign problem [10]. We set units such that $\hbar = k_B = m = 1$, and set the spatial lattice spacing to $\ell = 1$, which is equivalent to a choice of "lattice units." We use N to denote the total particle number, $N \equiv N_\uparrow + N_\downarrow$, where N_σ is the number of spin-σ particles with $\sigma \in \{\uparrow, \downarrow\}$, not to be confused with the particle number asymmetry $N_- \equiv N_\uparrow - N_\downarrow$.

Results. We determined the condensate fraction, critical temperature, spin susceptibility, even-odd pairing gap, and energy per particle. We also performed the first finite-temperature measurements of the Tan contact away from unitarity. Given the ongoing debate over pseudogap signatures and the relationship between the Tan contact, which is dominated by short-range interaction effects, and pairing, which characterizes long-range correlations (see Refs. [7, 16]), we defer these results to the supplementary material [9]. When comparing scattering lengths in a single plot, we use color to encode each scattering length as shown in the upper legend of Fig. 2. When comparing different lattice sizes, we encode each lattice size using marker shapes as shown in the legend of Fig. 1. Error bars on individual points represent statistical errors and show the standard error of the mean. Error bands in Figs. 3 and 4 incorporate statistical errors and finite volume effects and represent the standard error of the mean.

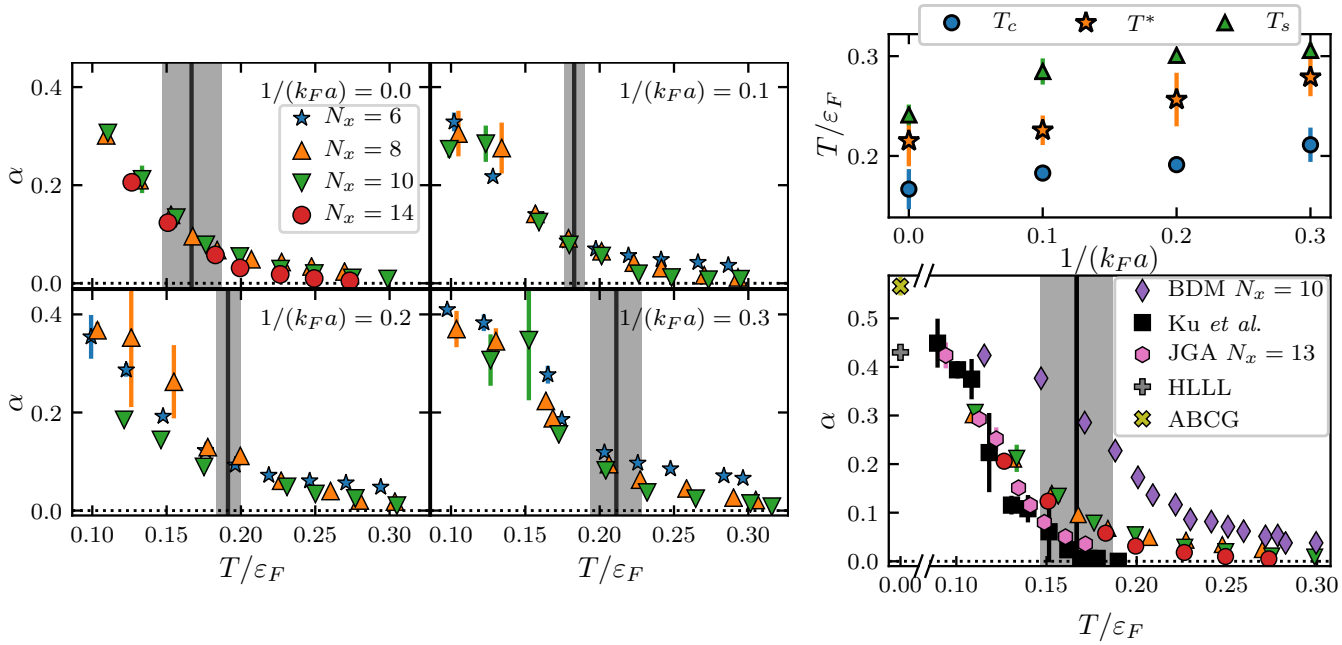

FIG. 1. Left: The condensate fraction α as a function of temperature at different scattering lengths; at a fixed temperature, α increases toward the BEC limit. Right (top): characteristic temperatures in the BCS–BEC crossover; T_c is the superfluid critical temperature; T_s is a lower bound on the temperature at which the spin susceptibility peaks; and T^* is the temperature at which the pairing gap disappears. Right (bottom): α at unitarity; our error bars are typically within the marker size. Also shown: the experimental results of Ku *et al.* [11] and the previous AFQMC studies of Bulgac *et al.* [12] (BDM) and Jensen *et al.* [13] (JGA). We also plot zero-temperature results by Astrakharchik *et al.* [14] (ABCG) and He *et al.* [15] (HLLL).

(i) The condensate fraction can be obtained from the asymptotic behavior of the quantity $h(r)$ [12, 14, 17]:

$$\alpha = \lim_{r\to\infty} h(r), \quad h(r) = \frac{N}{2}\left(g_2(r) - g_1(r)^2\right), \tag{1}$$

$$g_2(r) = \left(\tfrac{2}{N}\right)^2 \int \mathrm{d}^3\mathbf{r}_1\, \mathrm{d}^3\mathbf{r}_2 \left\langle \psi_\uparrow^\dagger(\mathbf{r}_1')\psi_\downarrow^\dagger(\mathbf{r}_2')\psi_\downarrow(\mathbf{r}_2)\psi_\uparrow(\mathbf{r}_1)\right\rangle,$$

$$g_1(r) = \tfrac{2}{N}\int \mathrm{d}^3\mathbf{r}_1 \left\langle \psi_\uparrow^\dagger(\mathbf{r}_1')\psi_\uparrow(\mathbf{r}_1)\right\rangle, \qquad \mathbf{r}_{1,2}' \equiv \mathbf{r}_{1,2} + \mathbf{r},$$

which acts as an order parameter, characterizing the extent of off-diagonal long-range order [18]. In Fig. 1, we show our results for α at different scattering lengths. An alternative approach is to estimate α as the maximum eigenvalue of g_2 [19]. Comparing our results to those of the eigenvalue method, and to experimental values in the right panel of Fig. 1, suggests that the eigenvalue method approaches the experimental α more quickly than our asymptotic value method, most noticeably at higher T.

However, we also use the finite-size scaling of α to determine T_c. By calculating α at multiple temperatures and lattice sizes, we obtain "crossing temperatures" (i.e. lattice-size-dependent estimates of T_c) from which we extrapolate to infinite volume to determine the true T_c [9, 12, 14, 17]. That procedure yields T_c as shown in Fig. 1, which are consistent with previous studies [12, 17] and in agreement with the experimental result $T_c/\varepsilon_F = 0.167(13)$ at unitarity [11].

(ii) A probe of the normal state character of the pairing is the spin-susceptibility χ_s, which should be suppressed below T^*, as fermions bind into pairs, making the gas strongly diamagnetic [24]. This is also naturally related to the fluctuations in particle asymmetry by

$$\chi_s = \frac{1}{TV}\left\langle \hat{N}_-^2 \right\rangle = \frac{1}{TV}\left\langle \left(\hat{N}_\uparrow - \hat{N}_\downarrow\right)^2 \right\rangle. \tag{2}$$

In Fig. 2, we show our results for χ_s. We use the particle-asymmetry constrained ensemble, which is completely sign-problem free [9]. Our results demonstrate an expected decrease in the maximal value of χ_s as $1/(k_F a)$ increases toward the BEC regime. We also find a moderate suppression of χ_s above T_c, which increases towards the BEC regime. In the lower panel of Fig. 2, we compare our results at unitarity to two previous AFQMC calculations [19, 20], an estimate using strong-coupling Luttinger-Ward theory [22], an experimental result from Sanner *et al.* [21], the prediction from normal Fermi liquid theory (nFLT), and a self-consistent NSR estimate from Pantel *et al.* [23]. The deviation from FLT behavior confirms symmetry based arguments by Rothstein and Shrivastava [25] that 3D unitary Fermi gases cannot be adequately described by nFLT in the range $T_c < T < T_F$. Our suppression in χ_s is less severe than in calculations by Wlazłowski *et al.* [20], supporting the argument by Jensen *et al.* [19] that said suppression is affected by the

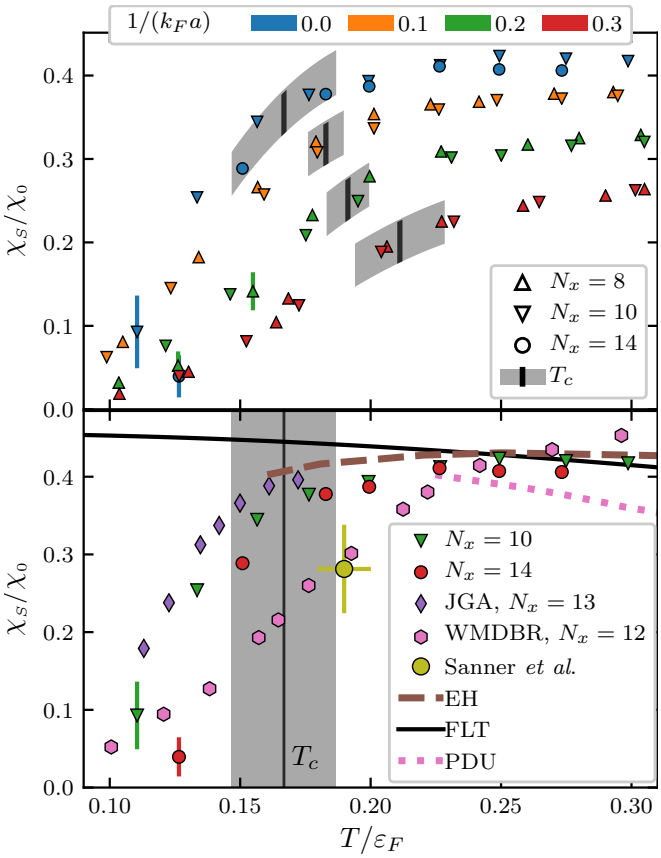

FIG. 2. Top: AFQMC results for the spin susceptibility χ_s at four different scattering lengths, scaled by its zero-temperature non-interacting counterpart, $\chi_0 = 3N/(2V\varepsilon_F)$. Bottom: At unitarity, we compare our result to two previous AFQMC studies: Jensen *et al.* [19] (JGA) and Wlazłowski *et al.* [20] (WMDBR); the experimental result of Sanner *et al.* [21]; a self-consistent Luttinger-Ward result (EH, [22]); the normal Fermi liquid theory prediction; and a self-consistent NSR result (PDU, [23]).

choice of spherical cutoff. However, our spin susceptibility is more suppressed than in both Jensen *et al.* and Enss and Haussmann [22], and, more importantly, the effect seems to grow for larger systems rather than lessen. Figure 2 also shows our results for the spin susceptibility for $0.1 \leq 1/(k_F a) \leq 0.3$. To our knowledge, these are the first QMC measurements of χ_s away from unitarity.

Tajima *et al.* [26, 27] identified the temperature at which χ_s peaks as T_s, and the temperature range $T_c < T < T_s$ as the "spin-gap" range where there are fewer free spins to contribute to χ_s. Although they find that $T_s \sim T^*$, the exact relationship between these two temperatures requires further study. We present only lower bounds for the temperature T_s in Fig. 1.

(iii) The even-odd staggering of systems with fixed particle numbers has been used as a measure of pairing since early studies of nuclear structure [28]. Several finite-difference formulas have been used to circumvent this (see Ref [29] for in-depth discussions). The simplest one is the three-point estimate, $\Delta_E^{(3)}$, which assumes a linear equation of state. If the equation of state has positive curvature, $\Delta_E^{(3)}$ will underestimate the pairing gap when N is even and overestimate the pairing gap when N is odd. Instead, we use the five-point expression

$$\Delta_E^{(5)} = \frac{(-1)^N}{8} \sum_{s=\pm 1} \Big[4E(N+s) - E(N+2s) - 3E(N) \Big], \quad (3)$$

where $E(N)$ is the ground state energy of a system with N total particles, which will be achieved when $|N_-| = \mathrm{mod}(N, 2)$. In addition to calculating $\Delta_E^{(5)}$, we propose another estimation method, which is to fit the energies calculated for many different values of N and N_- to a two-parameter equation of state,

$$\frac{E}{E_{FG}}(\xi, \Delta_E^{(f)}) = \xi + |N_-| \frac{\Delta_E^{(f)}}{E_{FG}}, \quad (4)$$

where $\xi(T/\varepsilon_F, 1/(k_F a))$ is a temperature-dependent generalization of the Bertsch parameter, $\varepsilon_F = (\hbar^2 k_F^2)/(2m)$ is the Fermi energy, $E_{FG} = 3N\varepsilon_F/5$ is the energy of a free Fermi gas at zero-temperature, and we use $|N_-| \in \{0, 1, 2\}$ for the fitting procedure [9]. Regardless of the estimation scheme, we expect Δ_E to become finite below some temperature T^*. If T^* exceeds the critical temperature T_c, this garners support for the existence of a pseudogap.

In Fig. 3, we present our results for the even-odd pairing gap, derived from both $\Delta_E^{(5)}$ and $\Delta_E^{(f)}$ [9]. In the lower panel, we compare our results at unitarity to previous theoretical and experimental studies: an AFQMC measurement of the spectral gap which employed a spherical momentum cutoff (MWB, [30]); a constrained ensemble AFQMC study (JGA, [19]) that estimated $\Delta^{(3)}$ with a cubic cutoff, but without relative temperature corrections, which we discuss in the supplement [9]; two low-temperature experimental results [32, 33]; and a zero-temperature QMC reference result [31]. We can view our results as charting a middle course between the Jensen *et al.* results and the Magierski *et al.* results, all of which can be interpreted as approaching the low-temperature reference results. However, the comparison is fraught since the spectral gap computed by Magierski *et al.* [30] is *a priori* a different quantity than the even-odd pairing gap and the critical temperature computed by Jensen *et al.* is lower than ours and also the experimentally determined value.

Despite the large uncertainties at low temperatures, we can appreciate certain features of the pairing gap. It is weaker, compared to the low temperature limit, for temperatures above T_c, however, it cannot be said to vanish immediately above the T_c error band even at unitarity.

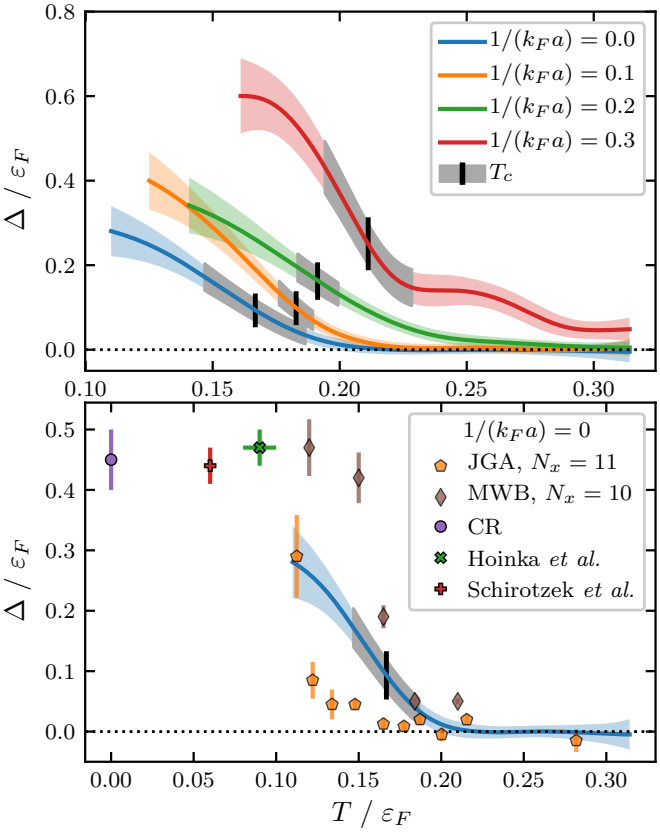

FIG. 3. Top: AFQMC results for Δ_E at four different scattering lengths, scaled by the Fermi energy ε_F. Bottom: At unitarity, we compare our results to the AFQMC results of Jensen *et al.* [19] (JGA) and Magierski *et al.* [30] (MWB); the zero-temperature QMC prediction of Carlson and Reddy [31] (CR); and the experimental results of Hoinka *et al.* [32] and Schirotzek *et al.* [33].

Our estimates for T^*, derived from spline fits [9] of both $\Delta_E^{(5)}$, see Eq. (3), and $\Delta_E^{(f)}$, see Eq. (4), are presented in Fig. 1 and are comparable with a previous AFQMC study that determined T^* from the spectral gap [30], as opposed to the even-odd energy gap [19].

(iv) Equation (4), which parameterizes the energies of systems with various numbers of $N_{\uparrow,\downarrow}$, also allows us to extract the temperature- and coupling constant-dependent Bertsch parameter $\xi(T/\varepsilon_F, 1/(k_F a))$. In Fig. 4 we show our results for $\xi(T/\varepsilon_F, 1/(k_F a))$ for each scattering length and compare to previous results. Similar to the results by Drut *et al.* [34] at unitarity, we did not capture the curvature in the equation of state seen by Ku *et al.* [11] below T_c. However, our results at unitarity do approach the reference values at zero temperature. We have a similar level of agreement with the results of Van Houcke *et al.* [37], which are not shown in Fig. 4, but are in excellent agreement with experiment in the normal state. We provide a table of values and errors for both ξ and Δ in the supplemental material [9].

Conclusion. We performed the first *ab initio* finite-temperature calculations of the spin susceptibility χ_s and Tan contact C away from unitarity, in addition to determining the condensate fraction α, the critical temperature T_c, the even-odd pairing gap Δ_E, and the Bertsch parameter ξ. For both the spin susceptibility and the even-odd pairing gap, we find no discontinuities as we reduce the coupling, but rather a smooth reduction in pseudogap signatures.

Since the BCS–BEC crossover is smooth, we do not expect an abrupt and discontinuous emergence of the pseudogap. Questions about where the pseudogap emerges are therefore analogous to long-debated questions about where the Earth's atmosphere ends [38]. Since the field is young, we have not yet developed the pseudogap analog of the Kármán line from space science. We have provided context to this discussion by looking for signatures of the pseudogap between $0.0 \leq 1/(k_F a) \leq 0.3$. At $1/(k_F a) = 0.3$, we see strong pseudogap signatures, which diminish towards unitarity. However, all characteristic temperatures T^* in Fig. 1 exceed the critical temperature T_c at all scattering lengths. Based on our results, we conclude it is premature to exclude unitarity from the pseudogap regime. Future work should include more refined extrapolations to the limit of zero-effective range, infinite volume, and zero density.

Acknowledgments.- We thank G. Wlazłowski for his valuable input and K. Roche and S. Jin for their guidance on the computational implementation. ARH and AB were supported by U.S. Department of Energy, Office of Science, Grant No. DE-FG02-97ER41014. ARH was also supported by the U.S. Department of Energy, Computa-

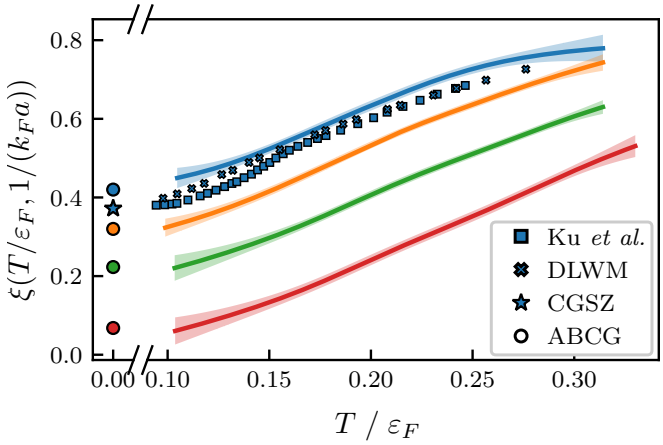

FIG. 4. AFQMC results for the temperature-dependent Bertsch parameter, $\xi(T/\varepsilon_F, 1/(k_F a))$ at four different scattering lengths. At unitarity, we compare our results to the experimental measurements of Ku *et al.* [11] and the high-precision AFQMC results of Drut *et al.* [34] (DLWM). We also show the zero temperature predictions of Carlson *et al.* [35] (CGSZ) at unitarity and of Astrakharchik *et al.* [36] (ABCG) at all scattering lengths.

tional Science Graduate Fellowship, under Grant No. DE-FG02-97ER25308. JD was supported by the U.S. National Science Foundation under Grant No. PHY1452635. This research used resources of the Oak Ridge Leadership Computing Facility, which is a US DOE Office of Science User Facility supported under Contract No. DE-AC05-00OR22725. This work was supported by "High Performance Computing Infrastructure" in Japan, Project ID: hp180048. A series of simulations were carried out on the Tsubame 3.0 supercomputer at Tokyo Institute of Technology. It was also facilitated through the use of advanced computational, storage, and networking infrastructure provided by the Hyak supercomputer system and funded by the STF at the University of Washington.

* richford@uw.edu
† drut@email.unc.edu
‡ bulgac@uw.edu

[1] W. Zwerger, *The BCS–BEC Crossover and the Unitary Fermi Gas* (Springer-Verlag, Berlin, 2012).
[2] G. C. Strinati, P. Pieri, G. Röpke, P. Schuck, and M. Urban, The BCS–BEC crossover: From ultra-cold Fermi gases to nuclear systems, Physics Reports **738**, 1 (2018).
[3] I. Bloch, J. Dalibard, and W. Zwerger, Many-body physics with ultracold gases, Rev. Mod. Phys. **80**, 885 (2008).
[4] S. Giorgini, L. P. Pitaevskii, and S. Stringari, Theory of ultracold atomic Fermi gases, Rev. Mod. Phys. **80**, 1215 (2008).
[5] C. Chin, R. Grimm, P. Julienne, and E. Tiesinga, Feshbach resonances in ultracold gases, Rev. Mod. Phys. **82**, 1225 (2010).
[6] Q. Chen, J. Stajic, S. Tan, and K. Levin, BCS–BEC crossover: From high temperature superconductors to ultracold superfluids, Physics Reports **412**, 1 (2005).
[7] E. J. Mueller, Review of pseudogaps in strongly interacting Fermi gases, Reports on Progress in Physics **80**, 104401 (2017).
[8] A. Bulgac, M. M. Forbes, and P. Magierski, The Unitary Fermi Gas: From Monte Carlo to Density Functionals, in *The BCS–BEC Crossover and the Unitary Fermi Gas*, edited by W. Zwerger (Springer Berlin Heidelberg, Berlin, Heidelberg, 2012) pp. 305–373.
[9] A. Richie-Halford, J. E. Drut, and A. Bulgac, See ancillary material on arXiv. (2020).
[10] C. E. Berger, L. Rammelmüller, A. C. Loheac, F. Ehmann, J. Braun, and J. E. Drut, Complex Langevin and other approaches to the sign problem in quantum many-body physics (2019), arXiv:1907.10183 [cond-mat.quant-gas].
[11] M. J. H. Ku, A. T. Sommer, L. W. Cheuk, and M. W. Zwierlein, Revealing the Superfluid Lambda Transition in the Universal Thermodynamics of a Unitary Fermi Gas, Science **335**, 563 (2012).
[12] A. Bulgac, J. E. Drut, and P. Magierski, Quantum Monte Carlo simulations of the BCS–BEC crossover at finite temperature, Phys. Rev. A **78**, 023625 (2008).
[13] S. Jensen, C. N. Gilbreth, and Y. Alhassid, Pairing Correlations across the Superfluid Phase Transition in the Unitary Fermi Gas, Phys. Rev. Lett. **124**, 090604 (2020).
[14] G. E. Astrakharchik, J. Boronat, J. Casulleras, and S. Giorgini, Momentum Distribution and Condensate Fraction of a Fermion Gas in the BCS–BEC Crossover, Phys. Rev. Lett. **95**, 230405 (2005).
[15] R. He, N. Li, B.-N. Lu, and D. Lee, Superfluid Condensate Fraction and Pairing Wave Function of the Unitary Fermi Gas (2019), arXiv:1910.01257 [cond-mat.quant-gas].
[16] P. Pieri, A. Perali, and G. C. Strinati, Enhanced paraconductivity-like fluctuations in the radiofrequency spectra of ultracold Fermi atoms, Nature Physics **5**, 736 (2009).
[17] E. Burovski, E. Kozik, N. Prokof'ev, B. Svistunov, and M. Troyer, Critical Temperature Curve in BEC–BCS Crossover, Phys. Rev. Lett. **101**, 090402 (2008).
[18] C. N. Yang, Concept of Off-Diagonal Long-Range Order and the Quantum Phases of Liquid He and of Superconductors, Rev. Mod. Phys. **34**, 694 (1962).
[19] S. Jensen, C. Gilbreth, and Y. Alhassid, The pseudogap regime in the unitary Fermi gas, The European Physical Journal Special Topics **227**, 2241 (2019).
[20] G. Wlazłowski, P. Magierski, J. E. Drut, A. Bulgac, and K. J. Roche, Cooper Pairing Above the Critical Temperature in a Unitary Fermi Gas, Phys. Rev. Lett. **110**, 090401 (2013).
[21] C. Sanner, E. J. Su, A. Keshet, W. Huang, J. Gillen, R. Gommers, and W. Ketterle, Speckle Imaging of Spin Fluctuations in a Strongly Interacting Fermi Gas, Phys. Rev. Lett. **106**, 010402 (2011).
[22] T. Enss and R. Haussmann, Quantum Mechanical Limitations to Spin Diffusion in the Unitary Fermi Gas, Phys. Rev. Lett. **109**, 195303 (2012).
[23] P.-A. Pantel, D. Davesne, and M. Urban, Polarized Fermi gases at finite temperature in the BCS–BEC crossover, Phys. Rev. A **90**, 053629 (2014).
[24] N. Trivedi and M. Randeria, Deviations from Fermi-Liquid Behavior above T_c in 2D Short Coherence Length Superconductors, Phys. Rev. Lett. **75**, 312 (1995).
[25] I. Z. Rothstein and P. Shrivastava, Symmetry obstruction to Fermi liquid behavior in the unitary limit, Phys. Rev. B **99**, 035101 (2019).
[26] H. Tajima, T. Kashimura, R. Hanai, R. Watanabe, and Y. Ohashi, Uniform spin susceptibility and spin-gap phenomenon in the BCS–BEC-crossover regime of an ultracold Fermi gas, Phys. Rev. A **89**, 033617 (2014).
[27] H. Tajima, R. Hanai, and Y. Ohashi, Strong-coupling corrections to spin susceptibility in the BCS–BEC-crossover regime of a superfluid Fermi gas, Phys. Rev. A **93**, 013610 (2016).
[28] A. Bohr and B. R. Mottelson, *Nuclear Structure*, Vol. 1 (World Scientific Publishing Company, 1998).
[29] D. G. Madland and J. Nix, New model of the average neutron and proton pairing gaps, Nuclear Physics A **476**, 1 (1988); P. Möller and J. Nix, Nuclear pairing models, Nuclear Physics A **536**, 20 (1992); T. Duguet, P. Bonche, P.-H. Heenen, and J. Meyer, Pairing correlations. II. Microscopic analysis of odd-even mass staggering in nuclei, Phys. Rev. C **65**, 014311 (2001).
[30] P. Magierski, G. Wlazłowski, and A. Bulgac, Onset of a Pseudogap Regime in Ultracold Fermi Gases, Phys. Rev. Lett. **107**, 145304 (2011).
[31] J. Carlson and S. Reddy, Superfluid Pairing Gap in

Strong Coupling, Phys. Rev. Lett. **100**, 150403 (2008).

[32] S. Hoinka, P. Dyke, M. G. Lingham, J. J. Kinnunen, G. M. Bruun, and C. J. Vale, Goldstone mode and pair-breaking excitations in atomic Fermi superfluids, Nature Physics **13**, 943 (2017).

[33] A. Schirotzek, Y.-i. Shin, C. H. Schunck, and W. Ketterle, Determination of the Superfluid Gap in Atomic Fermi Gases by Quasiparticle Spectroscopy, Phys. Rev. Lett. **101**, 140403 (2008).

[34] J. E. Drut, T. A. Lähde, G. Wlazłowski, and P. Magierski, Equation of state of the unitary Fermi gas: An update on lattice calculations, Phys. Rev. A **85**, 051601 (2012).

[35] J. Carlson, S. Gandolfi, K. E. Schmidt, and S. Zhang, Auxiliary-field quantum Monte Carlo method for strongly paired fermions, Phys. Rev. A **84**, 061602 (2011).

[36] G. E. Astrakharchik, J. Boronat, J. Casulleras, and S. Giorgini, Equation of State of a Fermi Gas in the BEC-BCS Crossover: A Quantum Monte Carlo Study, Phys. Rev. Lett. **93**, 200404 (2004).

[37] K. Van Houcke, F. Werner, E. Kozik, N. Prokof'ev, B. Svistunov, M. J. H. Ku, A. T. Sommer, L. W. Cheuk, A. Schirotzek, and M. W. Zwierlein, Feynman diagrams versus Fermi-gas Feynman emulator, Nature Physics **8**, 366 (2012).

[38] R. F. Goedhart, *The never ending dispute: delimitation of air space and outer space*, Vol. 4 (Editions Frontieres, 1996); J. C. McDowell, The edge of space: Revisiting the Karman Line, Acta Astronautica **151**, 668 (2018).